ACS APPLIED MATERIALS & INTERFACES

Research Article

www.acsami.org

Monolithic Polymeric Aerogels with VOCs Sorbent Nanoporous Crystalline and Water Sorbent Amorphous Phases

Vincenzo Venditto,*[,†] Marina Pellegrino,[†] Rosa Califano,[†] Gaetano Guerra,[†] Christophe Daniel,[†] Luigi Ambrosio,[‡] and Anna Borriello*[,‡]

[†]Department of Chemistry and Biology, Nanomates Center and INSTM Research Unit, University of Salerno, via Giovanni Paolo II, 84084 Fisciano, SA, Italy

[‡]Institute for Polymers, Composites and Biomaterials, National Research Council of Italy, P.le Fermi,1, 80055 Portici Naples, Italy

Supporting Information

ABSTRACT: Monolithic syndiotactic polystyrene (s-PS) aerogels, formed by highly crystalline nanofibrils with a hydrophobic nanoporous-crystalline phase and a hydrophilic amorphous phase have been prepared and characterized. These aerogels, with a high degree of sulfonation of the amorphous phase and nearly negligible sulfonation of the crystalline phase, are obtained by treating physical gels exhibiting δ-clathrate form. With respect to unsulfonated nanoporous-crystalline polymeric aerogels, these new selectively sulfonated aerogels present the great advantage of a high water diffusivity and water uptake up to 600 wt %. This water uptake increases greatly the sorption kinetics of organic pollutants by the hydrophobic nanopores of the crystalline phase. For instance, for aerogels with a sulfonation of 10%, the diffusivity of a volatile organic compound (1,2-dichloroethane, DCE) from 10 ppm aqueous solution is more than 3 orders of magnitude higher than that for the unsulfonated aerogel and is very close to the DCE diffusivity in water.

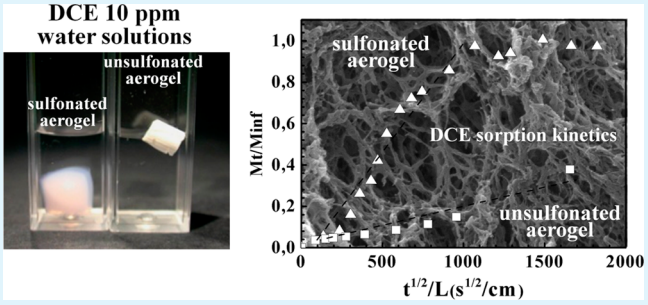

KEYWORDS: *syndiotactic polystyrene, solid-state sulfonation, nanoporous crystalline phase, water uptake, diffusivity*

INTRODUCTION

Aerogels are generally obtained by drying of wet gels and constitute a unique class of materials, which is characterized by highly porous networks. For many applications, it is relevant to obtain monolithic aerogels, which can be easily obtained with different organic/inorganic materials such as silica,[1−3] clays[4−6] and polymers.[7−22] The most common type of monolithic polymeric aerogels reported in literature are obtained with a large variety of chemically cross-linked polymers, such as resorcinol-formaldehyde,[7,8] melamine-formaldehyde,[9] polyurethane,[10] polyimide,[11] polyamide,[12] and also from polymeric organic framework (POF).[13] Robust monolithic polymeric aerogels can be also obtained from gels being formed through a three-dimensional network based on interchain ionic interactions or crystalline regions instead of covalent bonds. In particular, hydrophilic aerogels are obtained from hydrogels generally made of natural polysaccharides like cellulose,[14] alginates,[15,16] carrageenans,[15] chitosan,[15] or chitin[17] while hydrophobic aerogels with crystalline phases are obtained from organogels, generally based on regular synthetic polymers such as syndiotactic polystyrene,[18] poly(L-lactic acid),[19] poly(vinylidene fluoride),[20] poly(vinylidene fluoride-*co*-hexafluoropropylene),[21] and poly(4-methyl-1-pentene).[22]

In the two last decades, the formation of polymeric nanoporous-crystalline forms, that is, of crystalline forms presenting an ordered 3-D distribution of molecular-size cavities and exhibiting density lower than the corresponding amorphous forms, has been discovered.[23−25] In particular, nanoporous crystalline forms have been disclosed for two industrially relevant polymers: syndiotactic polystyrene (s-PS)[23,24] and poly(2,6-dimethyl-1,4-phenylene)oxide (PPO).[25] These nanoporous-crystalline polymers are able to absorb volatile organic compounds (VOCs) also when present in traces and have been proposed for molecular separation,[26−31] sensor,[32,33] and catalysis[34] applications.

Based on these thermoplastic polymers exhibiting nanoporous-crystalline forms, a special class of monolithic physically cross-linked aerogels, has been achieved. These nanoporous-crystalline polymeric aerogels, whose physical knots are constituted by nanoporous-crystalline phases, exhibit beside disordered amorphous meso and macropores (typical of all aerogels) all identical nanopores (or microporous according to IUPAC classification) of the crystalline phases.[18,35−38] Nanoporous-crystalline aerogels present the high sorption capacity typical of the nanoporous crystalline phases (due to the sorption of molecules as isolated guests of the host crystalline

Received: October 30, 2014
Accepted: December 22, 2014
Published: December 22, 2014

ACS Publications © 2014 American Chemical Society

DOI: 10.1021/am507116e
ACS Appl. Mater. Interfaces 2015, 7, 1318−1326

phase) associated with the high sorption kinetics typical of aerogels (due to the high and disordered porosity of the aerogels).[18,35−38] This gives high guest solubility particularly relevant for VOCs in traces as well as high selectivity, mainly due to specific host−guest interactions in crystalline phases. Moreover, low material cost, robustness, durability, and easy recycling of the used commercial thermoplastic polymers, associated with the ease of handling, make these aerogels suitable for applications in chemical separations (mainly air purification),[18,35−38] oil-spill recovery,[38] and gas (mainly hydrogen)[39] storage.

Nanoporous-crystalline polymeric materials, although characterized by high uptake and fast diffusivity of VOCs, present poor water permeability. This strongly reduces pollutant sorption kinetics and constitutes a major drawback for their practical use in water purification.

This inconvenience has been overcome, at least for s-PS films, by a selective solid-state sulfonation procedure, based on sulfonating agents being bigger than the polymer crystalline cavities.[40−42] This leaves essentially unaltered δ or ε nanoporous-crystalline phases while making highly hydrophilic the corresponding amorphous phases.[40−42] This procedure, however, is not suitable for s-PS aerogels which, after this sulfonation treatment, become mushy and are rapidly destroyed when soaked in water.

Sulfonated s-PS aerogels, have been recently obtained from gels prepared with sulfonated polymer, after extraction by $scCO_2$.[43] However, the extraction of gels of sulfonated s-PS leads to large and irregular shrinkages, at least for degree of sulfonation higher than 22%.[43]

In this paper, robust and high porosity monolithic s-PS aerogels, even for degrees of sulfonation as high as 30%, are obtained by sulfonation of s-PS organogels (rather than gelation of sulfonated s-PS). This procedure poorly affects the crystalline phase, leading to selective sulfonation of the amorphous polymer fraction. The main advantage of s-PS gels, sulfonated in the gel state, is the occurrence of negligible monolith shrinkage, when extracted by $scCO_2$.

The obtained hydrophilic-amorphous/hydrophobic-nanoporous-crystalline aerogels have been characterized by X-ray diffraction analysis, IR spectroscopy, scanning electron microscopy, and nitrogen sorption measurements, and their water uptake and diffusivity, as well as their sorption properties of VOCs from diluted aqueous solutions, have been investigated. In particular, sorption of 1,2-dichloroethane (DCE), an aquifers contaminant which presents high resistance to common remediation techniques based on reactive barriers containing Fe0[44] has been considered.

EXPERIMENTAL SECTION

Materials. The s-PS used in this study was manufactured by Dow Chemical Company under the trademark Questra 101. The ^{13}C nuclear magnetic resonance characterization showed that the content of syndiotactic triads was over 98%. The weight-average molar mass obtained by gel permeation chromatography (GPC) in trichlorobenzene at 135 °C was found to be $M_w = 3.2 \times 10^5$ with the polydispersity index, $M_w/M_n = 3.9$. All solvents and reagents were purchased from Aldrich and used without further purification.

Gels Preparation Procedure. All semicrystalline gels considered in this paper have been obtained by dissolving s-PS pellets in chloroform or 1,2-dichloroethane (solvent/polymer ratio of 90/10 by weight) in hermetically sealed test tube above the solvent boiling temperature. After complete dissolution of the polymer, the hot solution was cooled to room temperature and gelation occurred.

Sulfonation Procedure. The sulfonating reagent was prepared by mixing an excess of dodecanoic acid (lauric acid) with chlorosulfonic acid ($ClSO_3H$) at room temperature, for 24 h. In particular a mixture of 4.8×10^{-2} mol of lauric acid (≥98%) for 3.0×10^{-2} mol of $ClSO_3H$ (99%) was used.

s-PS gel cylinders with a diameter of ca. 6 mm, length of ca. 35 mm and weight of ca. 1.5 g were immersed in solutions containing a given amount of sulfonating reagent and 40 mL of chloroform or 1,2-dichloroethane depending on the solvent used for the gel preparation for a time sufficient to the gel swelling with sulfonating reagent (≈ 12 h). The swelled s-PS gel cylinders were removed from the sulfonating solution and soaked in pure chloroform or DCE and the sulfonation reaction was thermally activated by heating at $T = 40$ °C. Samples with different sulfonation degrees were obtained by changing the heating times and the amount of sulfonating reagent in the solution (i.e., 2 g of sulfonating reagent and 1 h heating time to obtain an aerogel with a degree of sulfonation of 3.5%).

The resulting sulfonated gels were purified from possible residuals of the sulfonation process by washing the gels with ethanol and pure chloroform or DCE and the sulfonated aerogels were finally obtained by extracting the solvent with $scCO_2$. The absence of any residuals in the aerogels was verified by FTIR (see Figure S1 in the Supporting Information).

The solvent extraction was performed by using a SFX 200 supercritical carbon dioxide extractor (ISCO Inc.) under the following conditions, $T = 40$ °C, $P = 200$ bar, extraction time $t = 180$ min. This procedure allows a complete removal of possible guest molecules from all possible s-PS cocrystalline phases, leading to nanoporous crystalline phases.[18,35−37]

For monolithic aerogels with a regular shape (i.e., spherical or cylindrical), the total porosity, including macroporosity, mesoporosity, and microporosity, can be estimated from the volume/mass ratio of the aerogel. Then, the percentage of porosity P of the aerogel samples can be expressed as

$$P = 100\left(1 - \frac{\rho_{app}}{\rho_{pol}}\right) \quad (1)$$

where ρ_{pol} is the density of the polymer matrix and ρ_{app} is the aerogel apparent density calculated from the mass/volume ratio of the monolithic aerogels.

Techniques. Micrographs are obtained by using a scanning electron microscope (SEM) (Leica Cambridge Stereoscan S440) coupled with a probe for energy-dispersive scanning (EDS), to evaluate the sulfonation degree at different depths throughout the sample thickness. The aerogels were cryogenically fractured in liquid N_2 for the SEM-EDS experiments in order to gain access to the internal part of the samples. Before imaging, all the specimens were coated with gold using a VCR high resolution indirect ion-beam sputtering system.

Wide-angle X-ray diffraction patterns with nickel filtered Cu Kα radiation were obtained, in reflection, with an automatic Bruker D8 Advance diffractometer.

A crystallinity index (X_c) has been determined resolving the X-ray diffraction pattern in a selected 2θ range (5−40°), into two areas A_c and A_a that can be taken as proportional to the crystalline and amorphous weight fractions, respectively, and calculated trough the expression

$$X_c = [A_c/(A_c + A_a)]100$$

Infrared spectra were obtained at a resolution of 2.0 cm^{-1} with a Tensor 27 Bruker spectrometer equipped with deuterated triglycine sulfate (DTGS) detector and a Ge/KBr beam splitter. The frequency scale was internally calibrated to 0.01 cm^{-1} using a He−Ne laser; 32 scans were signal averaged to reduce the noise.

DCE equilibrium sorption isotherms from aqueous solutions were obtained by measurements of FTIR absorbances of DCE peaks using calibration curves analogous to those described in ref 45.

DOI: 10.1021/am507116e
ACS Appl. Mater. Interfaces 2015, 7, 1318−1326

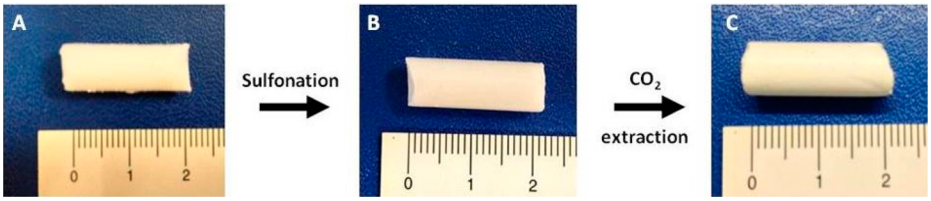

Figure 1. Photographs of a piece of s-PS gel prepared in 1,2-dichloroethane at C_{pol} = 0.10 g/g, before (A) and after (B) sulfonation. The photograph of the corresponding sulfonated aerogel, as obtained by complete solvent extraction via $scCO_2$ is shown in C. Units of the ruler are centimeters.

Nitrogen adsorption at liquid nitrogen temperature (77 K) was used to measure surface areas of unsulfonated and sulfonated aerogels with a Nova Quantachrome 4200e instrument. Before the adsorption measurement, aerogel samples were degassed at 45 °C under vacuum for 24 h. The surface area values were calculated using the Brunauer–Emmet–Teller (BET) method.

The water uptake of the polymers was investigated by a Q5000 SA thermogravimetric analyzer from TA Instruments, containing a microbalance in which the sample and reference pans were enclosed in a temperature and humidity controlled chamber. The temperature in the Q5000 SA was controlled by Peltier elements. Dried N_2 gas flow (200 mL min^{-1}) was split into two parts, of which one part was wetted by passing it through a water-saturated chamber.

The aerogel sulfonation degree has been determined by elemental analysis of whole aerogel sections using a Flash EA 1112 analyzer from Thermo Fisher Scientific and the reported sulfonation degree (thereafter indicated as S) is reported as a molar percent of sulfonated monomeric units.

$$S = (\text{sulfur moles by elemental analysis} / \text{moles of polymer styrenic units}) 100$$

RESULT AND DISCUSSION

Preparation of Monolithic Aerogels with Sulfonated Amorphous Phase. In a recent paper, we have described a procedure for solid-state sulfonation of syndiotactic polystyrene semicrystalline films involving the use of a bulky sulfonating agent (lauroyl sulfate), which was effective to selectively react with the phenyl rings of the polymer amorphous phase, leaving substantially unaltered the crystalline phase.[40]

Based on this experience, the same sulfonation procedure was applied on s-PS aerogels obtained after solvent extraction of s-PS/chloroform gels in order to obtain aerogels with sulfonated amorphous phases.

However, the direct sulfonation of aerogels, exhibiting the δ and ε nanoporous crystalline s-PS forms or the dense β s-PS form and having porosity less than 80%, is not useful because the corresponding sulfonated aerogels, although remaining monolithic and stable in organic solvent totally break up when soaked in water.

For this reason, a new appropriate sulfonation procedure, reported in detail in the Experimental Section, has been developed. In this procedure, the treatment with the sulfonating agent is carried out on gels rather than on aerogels. Then, sulfonated aerogels can be obtained from sulfonated gels using the typical solvent extraction by $scCO_2$.

The sulfonation procedure has been carried out with s-PS gels with chloroform and 1,2-dichloroethane (DCE). As an example, the photographs of a piece of s-PS gel prepared in DCE at a polymer concentration Cpol = 0.10 g/g, before and after sulfonation and of the corresponding aerogel, as obtained by complete solvent extraction by $scCO_2$, are shown in Figure 1.

Figure 1 clearly shows that the dimensions of the gel remain substantially unchanged during the sulfonation and extraction procedures and that a monolithic aerogel is obtained. The values of aerogel apparent porosity reported in Table 1

Table 1. Areogel Apparent Porosity, Crystalline Degree Evaluated from X-ray Diffraction Patterns, BET Values of Aerogels with Different Degree of Sulfonation Prepared from 1-2-Dichloroethane (DCE) and Chloroform

solvent	sulfonation degree (S) (%)	porosity (%)	crystalline degree (X-ray, %)	BET (m^2/g)
DCE	0	88	40	220
DCE	4	89	30	214
DCE	9.5	85	23	193
DCE	16	87	10	171
DCE	19	89	8	177
$CHCl_3$	0	92	45	284
$CHCl_3$	7.5	80	35	245
$CHCl_3$	12	80	30	n.d.
$CHCl_3$	20.5	79	15	150
$CHCl_3$	32	82	10	150

(column 3, lines 2–5) for aerogels with different degree of sulfonation show that at least for sulfonation degree up to 20%, the porosity of the sulfonated aerogels obtained from s-PS/DCE gel is nearly equal to those of the corresponding unsulfonated aerogels (i.e., nearly 90%, for the considered solvent/polymer 90/10 ratio). Unlike DCE, a small decrease of the aerogel porosity occurs when the sulfonation procedure is carried out on s-PS gels in chloroform as can be seen in Table 1 (column 3, lines 8–12). For example, in this case, the porosity of sulfonated aerogels for sulfonation degree S = 20.5% is 79%, while the porosity of the unsulfonated aerogels is 92% as can be seen in Table 1.

In this respect, it is worth adding that, when aerogels are obtained from gels of sulfonated s-PS, a large and irregular shrinkage of the aerogels is observed for sulfonated s-PS with degree of sulfonation of 22%.[43]

Typical SEM micrographs of a unsulfonated aerogel and of a sulfonated aerogel with a degree of sulfonation of 12% being obtained from gels prepared in chloroform at C_{pol} = 0.1 g/g are reported in Figure 2A and B, respectively.

Figure 2 shows that the gel-state sulfonation procedure does not modify the gel morphology, maintaining the typical nanofibrillar morphology previously reported for most unsulfonated s-PS aerogels.[18,36,38] The morpholology steadiness was also observed for DCE-based aerogels as shown in Figure S2 of the Supporting Information.

Structural Characterization of Sulfonated s-PS Aerogels. The X-ray diffraction patterns of unsulfonated and sulfonated s-PS aerogels with a degree of sulfonation up to ca. *S* = 20% being obtained from gel preparation and sulfonation

DOI: 10.1021/am507116e
ACS Appl. Mater. Interfaces 2015, 7, 1318–1326

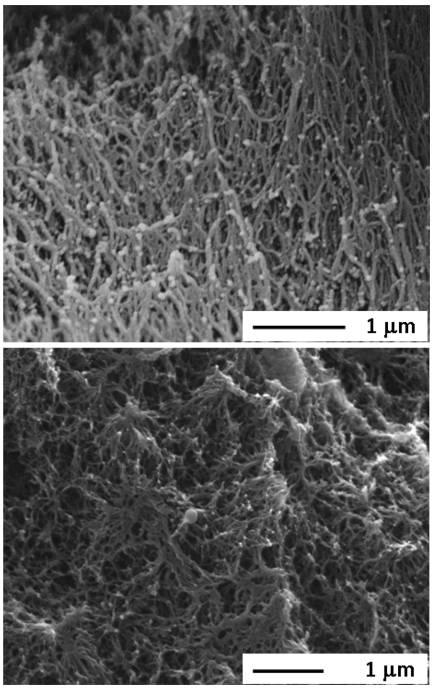

Figure 2. SEM micrographs of an unsulfonated aerogel (up) and of a sulfonated aerogel with S = 12% (down) being obtained from gels prepared in chloroform at C_{pol} = 0.1 g/g.

procedure carried out with chloroform and DCE are reported in Figure 3A and B, respectively.

We can observe that both unsulfonated aerogels present strong reflections located at 2θ (X-ray wavelength corresponding to Cu Kα emission) 8.3, 13.5, 16.8, 20.7, 23.5° being typical of the s-PS δ nanoporous crystalline form.[23] The degree of crystallinity, as evaluated by subtraction of the amorphous halo, for unsulfonated aerogels obtained in chloroform and DCE is 40% and 45%, respectively.

The X-ray diffraction patterns of sulfonated aerogels show that all samples are semicrystalline, and in particular, the diffraction patterns still present a diffraction peak located at 2θ ~ 8.3, which indicates the existence of the nanoporous delta form in the sulfonated aerogels.

The diffraction patterns also clearly show a progressive decrease of the degree of crystallinity with increasing the degree of sulfonation (see Table 1, column 4). For example, while the crystallinity degree estimated by subtraction of the amorphous diffraction pattern is equal to 45% for the unsulfonated aerogel obtained in chloroform (S = 0% in Figure 3A), it decreases to 30% for an aerogel with a degree of sulfonation of 12%.

It is also worth noting that the aerogels obtained with a chloroform preparation procedure present a higher degree of crystallinity than aerogels obtained from DCE.

Thus, an aerogel with S = 20.5% obtained with chloroform (Figure 3A) presents a degree of crystallinity of ca. 15% while the aerogel with the same degree of sulfonation being obtained with DCE presents a degree of crystallinity of ca. 8% (Figure 3B).

FTIR spectra in the wavenumber ranges 1300−980 cm^{-1} and 590−480 cm^{-1} of unsulfonated and sulfonated aerogels, whose X-ray diffraction patterns are shown in Figure 3, are reported in Figure 4.

As expected, a progressive increase of the 1126 cm^{-1} (in-plane vibrations of disubstituted aromatic rings)[46] and 1007 cm^{-1} (in-plane bending deformation of the aromatic ring substituted with a sulfonic acid group)[46] peaks with increasing the aerogel degree of sulfonation is observed. It is also worth noting that another IR band located at 1412 cm^{-1}, absent in unsulfonated s-PS and never described for sulfonated polystyrenes, also increases with increasing the sulfonation degree.

The FTIR spectra of unsulfonated s-PS aerogels obtained in chloroform and DCE present infrared bands at 1277, 572, and 502 cm^{-1} being characteristic of the ordered s(2/1)2 helical conformation of the s-PS nanoporous δ crystalline form. It is also worth noting that the absorbance of the characteristic bands of the ordered helical conformation is higher for aerogels obtained from chloroform than from DCE. This result is consistent with the X-ray diffraction patterns reported in Figure 4.

The absorbance of these helical conformation bands decreases progressively with increasing the degree of sulfonation which indicates a decrease of the polymer fraction with ordered s(2/1)2 helical conformation. However, this decrease is much less pronounced that the decrease of the crystalline degree evaluated from X-ray diffraction patterns. In particular, for aerogels obtained with DCE, the X-ray diffraction crystalline degree for the aerogel with S ~ 19% is ca. 5 times lower than for the unsulfonated aerogel (40% vs 8%, Table 1,

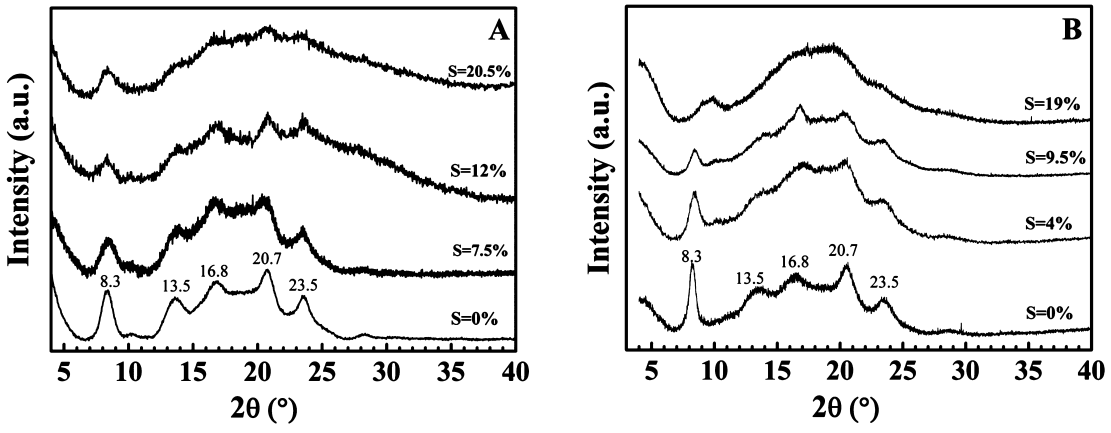

Figure 3. X-ray diffraction patterns (Cu Kα) of unsulfonated and sulfonated aerogels presenting different degree of sulfonation obtained using chloroform (A) and DCE (B), for both gel preparation and sulfonation processes.

DOI: 10.1021/am507116e
ACS Appl. Mater. Interfaces 2015, 7, 1318−1326

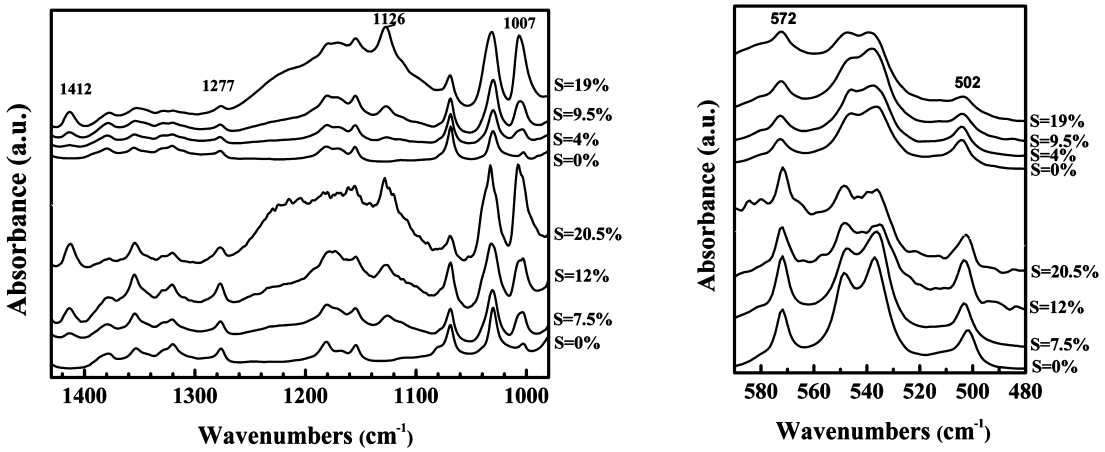

Figure 4. FTIR spectra, in the wavenumber ranges 1430−980 cm^{-1} (left) and 590−480 cm^{-1} (right) of unsulfonated and sulfonated s-PS aerogels exhibiting nanoporous crystalline δ form obtained in chloroform (bottom curves) and DCE (top curves). Relevant absorbance peaks associated with the crystalline (1277, 572, and 502 cm^{-1}) δ form or with the sulfonation level (1126 and 1007 cm^{-1}) are also indicated. The degree of sulfonation, evaluated by the elemental analysis, is reported near the curves.

column 4), while the normalized absorbance of the s(2/1)2 helical band located at 572 cm^{-1} for the aerogel with S ∼ 19% is ca. 2 times lower than for the unsulfonated aerogel.

This difference can be explained by the formation of smaller crystallites during sulfonation. As X-ray diffraction affords a determination of long-range three-dimensional order while infrared spectroscopy affords a determination of short-range, conformational order, the degree of crystallinity evaluated by FTIR spectroscopy is not affected by the dimension and the perfection of the crystallites and thus is generally larger than the degree of crystallinity evaluated by X-ray diffraction.[47]

Thus, it is possible to conclude from combined FTIR and X-ray diffraction analysis that (i) only s-PS chains of the amorphous phase are sulfonated and (ii) the sulfonation leads to a decrease of the aerogel crystalline degree but there are still a meaningful amount of small nanoporous δ-form crystals for degree of sulfonation as high as 20%.

Surface Area Characterization of Sulfonated Aerogels. The BET surface areas of aerogels determined from nitrogen adsorption isotherms at 77 K are compared in Table 1 (column 5) and in Figure 5 for unsulfonated and sulfonated aerogels obtained from gels prepared in chloroform and DCE.

Figure 5 clearly shows that for aerogels, both from DCE and chloroform, the BET decreases with the degree of sulfonation.

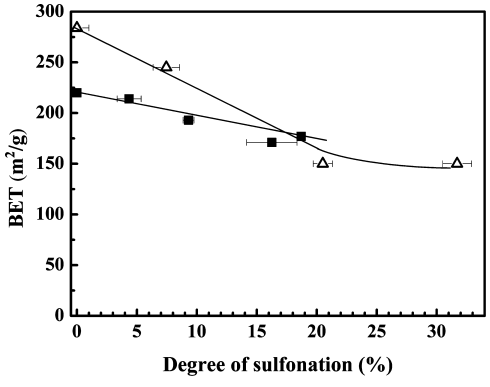

Figure 5. Surface area (BET, m^2/g) of s-PS aerogels with different degree of sulfonation obtained using chloroform (Δ) and DCE (■) for both gel preparation and sulfonation processes.

In s-PS samples with the δ nanoporous crystalline phase the BET values depend on the degree of crystallinity (i.e., amount of crystalline nanopores) but also on the apparent porosity (i.e., accessibility of the crystalline nanopores).[35]

As mentioned above, the degree of crystallinity evaluated by X-ray diffraction is underestimated when small crystallites are present, and thus, the BET values cannot be directly correlated to the crystallinity values reported in Table 1, column 4, which have been obtained by the subtraction of the amorphous halo from the diffraction pattern. The decrease of the BET values observed for sulfonated aerogels is better correlated with the decrease of the short-range conformational order measured by FTIR spectroscopy. The better qualitative correlation between the decrease of the BET values and the decrease of s(2/1)2 helical absorbance band is shown in Figure S3 of the Supporting Information.

In particular for sulfonated aerogels obtained from DCE, the apparent porosities for unsulfonated and sulfonated aerogels are substantially unchanged (i.e., P = 90%) and thus the BET decrease should only be due to a decrease of the short-range conformational order. As the absorbance of the s(2/1)2 helical band located at 572 cm^{-1} for the aerogel with S ∼ 19% is ca. 2 times lower than for the unsulfonated aerogel, by considering that the BET value of a s-PS aerogel with the same porosity but without crystalline nanopores is ca. 65 m^2/g,[37] the estimated calculated BET value for the aerogel with S ∼ 19% is ca. 150 m^2/g. This value is consistent with the BET measured value, which is 177 m^2/g.

For aerogels obtained from chloroform, the larger decrease of the BET can be attributed to a decrease of both the crystalline order and the apparent porosity.

Despite the progressive BET decrease with increasing sulfonation degree, it is worth emphasizing that the innovative sulfonation process reported here allows the preparation of monolithic aerogels characterized by the nanoporous δ-form, a sulfonation degree larger than 30%, an apparent porosity of 80% and high BET values of ca. 150 m^2/g.

Sorption Properties of Sulfonated s-PS Aerogels. *Water Sorption.* Syndiotactic polystyrene is a completely hydrophobic polymer while semicrystalline nanoporous s-PS samples with a selective sulfonated amorphous phase presents a

DOI: 10.1021/am507116e
ACS Appl. Mater. Interfaces 2015, 7, 1318−1326

highly hydrophilic amorphous phase and at the same time an hydrophobic nanoporous-crystalline phase.

The different floating behavior of unsulfonated and sulfonated (S = 20%) s-PS aerogels, when soaked in water is shown in Figure 6.

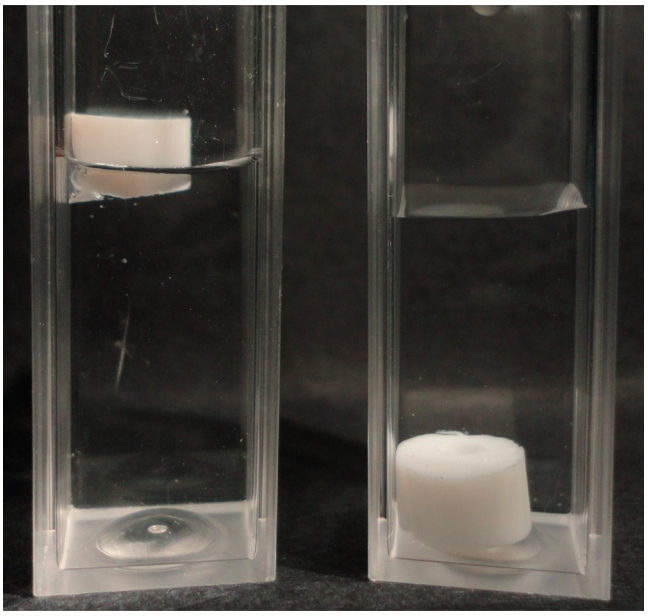

Figure 6. Sulfonated (right) and unsulfonated (left) s-PS aerogels immersed in water.

In previous reports,[40,42] it has been shown that the solid-state selective sulfonation of the amorphous phase in semicrystalline films characterized by the nanoporous δ crystalline form can lead to hydrophilic films characterized by a high water uptake. The liquid water uptake of sulfonated s-PS films and sulfonated aerogels obtained from chloroform and DCE are compared in Figure 7A.

We can observe that, as already observed with films, the water uptake in sulfonated aerogels increases with increasing degree of sulfonation. The larger water uptake observed with sulfonated aerogels with respect to sulfonated films with the same sulfonation degree is due to the highly amorphous porous structure (i.e., mesopores and macropores) of the aerogels.

It should also be emphasized that only a small aerogel swelling occurs during the water uptake. As an example, aerogels with sulfonation degree of 20% have a volume change lower than 10%.

Figure 7A also shows that the water uptake for aerogels being obtained with DCE is larger than that for aerogels obtained from chloroform. This result can be attributed to the higher apparent porosity of the DCE-based aerogels but other aerogel microstructure characteristics such as more uniform and smaller pore size and higher degree of interconnections may also play a role.[48]

The water sorption kinetics at 0.8 water vapor activity for a sulfonated film (S = 26%) and a sulfonated aerogel (S = 15%), both obtained from chloroform, are shown in Figure 7B. The reported curves clearly show that the aerogel presents a sorption kinetic faster than for the film, despite of the lower sulfonation degree. In particular, the water apparent diffusion Fick coefficients (D_{app}), obtained from the slopes of the linear region (Mt/Minf < 0.5) of the sorption curves,[49] of the analyzed s-PS film and sulfonated aerogel samples are 3.9 × 10^{-9} cm^2/s and 2.3 × 10^{-6} cm^2/s, respectively.

It is worth noting that the observed value of the water diffusion coefficient in sulfonated s-PS aerogels (S = 15%) is in agreement with the apparent diffusion Fick's coefficients commonly observed in polymeric hydrogels.[50,51]

VOCs Sorption from Diluted Aqueous Solutions. The sorption capacity of VOCs both from vapor phase or diluted aqueous solutions in s-PS aerogels has been largely investigated.[18,35−38]

In particular, the DCE sorption uptake from diluted aqueous solutions has been extensively studied as a result of its presence as pollutant in contaminated aquifers. Moreover, DCE is characterized by a selective sorption of DCE *trans* conformer into the s-PS nanoporous crystalline δ form,[45,52] which allows, from the infrared analysis of DCE conformers, a simple quantitative evaluation of fraction of DCE sorbed in the nanoporous crystalline δ form (only *trans* conformer) or in the amorphous phase (both *trans* and *gauche* conformers).[45,52]

FTIR spectra in the wavenumber range 1300−1100 cm^{-1} of a sulfonated δ-aerogel with porosity P = 89% and S = 10%, soaked in a 10 ppm DCE aqueous solution for different times, are reported in Figure 8.

In these FTIR spectra, only the peak of the DCE *trans* conformer at 1234 cm^{-1} is present, while the peak of the DCE

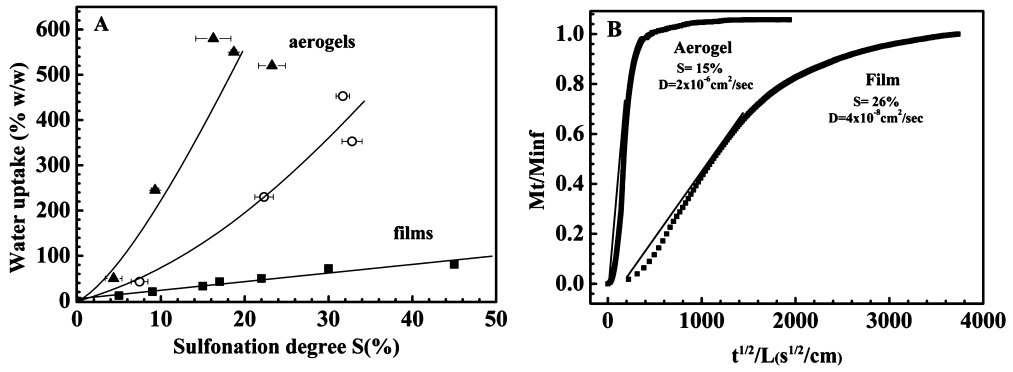

Figure 7. (A) Liquid water sorption, as a function of sulfonation degree, from s-PS nanoporous crystalline sulfonated monolithic aerogels obtained from DCE (▲), chloroform (○), and films (■). (B) Water sorption kinetics at room temperature and at 0.8 water vapor activity, from a sulfonated s-PS film with S = 25% and an aerogel with S = 15%, obtained from chloroform. Mt and Minf are the water uptake at time t and equilibrium, respectively, and L is the macroscopic thickness of aerogel.

DOI: 10.1021/am507116e
ACS Appl. Mater. Interfaces 2015, 7, 1318−1326

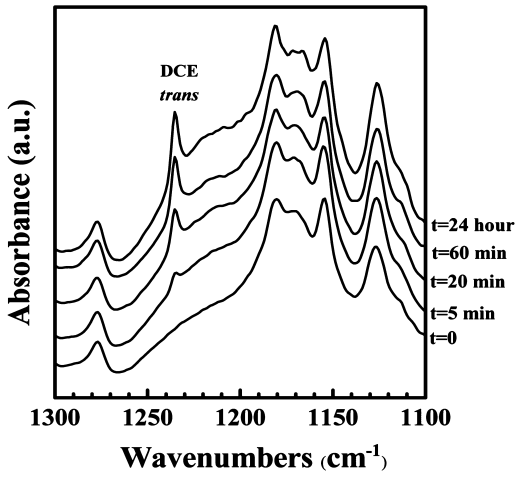

Figure 8. FTIR spectra of a sulfonated δ-aerogel with P = 89% and S = 10% soaked in a 10 ppm DCE aqueous solution for different times.

gauche conformer at 1284 cm^{-1} is absent. This shows that most DCE molecules are guest of the nanoporous δ crystalline phase.[45,52]

From the absorbance peaks of the DCE *trans* conformer the equilibrium uptake of DCE in the sulfonated aerogel with S = 10% was found to be 3.2 wt %. It is worth noting that this value is somewhat lower than the equilibrium uptake for the corresponding unsulfonated aerogels (ca. 5 wt %).[35] This decrease of DCE uptake can be correlated to the decrease of the crystalline degree (Figure 3B and Table 1).

DCE sorption kinetics of δ-form unsulfonated aerogels with a porosity P = 90% and δ-form sulfonated aerogel obtained from DCE with a porosity P = 89% and a degree of sulfonation S = 10% from 100 ppm (A) and 10 ppm (B) solutions, as obtained by FTIR measurements, are compared in Figure 9.

We can clearly observe a significant increase of the sorption kinetics for the sulfonated aerogel, and this increase appears to be more pronounced when the VOC concentration in the aqueous solution is reduced. Thus, for a 10 ppm solution, at $t^{1/2}/L$ = 1000, which corresponds to a sorption time of ca. 3 hours with an aerogel of macroscopic thickness of 1 mm, the sulfonated aerogel has already sorbed ca. 90% of its equilibrium uptake (i.e., 2.9 wt % for an equilibrium uptake of 3.2 wt %) while the unsulfonated aerogel has sorbed only 15% of the equilibrium uptake (i.e., 0.75 wt % for an equilibrium uptake of ca. 5 wt %). Thus, sulfonated aerogels are more efficient than unsulfonated aerogels for short sorption times.

As already established in previous papers[27,29,45] the kinetic curves for guest sorption into the s-PS nanoporous crystalline δ-phase samples can be fitted by means of Fick's model. The apparent diffusivity constants (D_{app}) obtained by the slopes of the initial linear region of the sorption curves of unsulfonated and sulfonated aerogels[49] are reported in Table 2 and added as labels to the curves in Figure 9A and B.

Table 2. Apparent Diffusivity Constants at Room Temperature and Equilibrium Uptake of DCE into s-PS δ from Aerogel Samples Having Different Porosity and Sulfonation Degree, for Sorption from Different DCE Diluted Aqueous Solutions

P (%)	DCE concn. (ppm)	S (%)	Dapp (cm^2/s)	DCE uptake (wt %)
90	100	0	2×10^{-7}	7
89	100	10	2.1×10^{-5}	5.6
90	10	0	2.4×10^{-9}	5
89	10	10	5.1×10^{-6}	3.2

It is clearly evident that the DCE apparent diffusivity constant substantially increases after sulfonation of the aerogels. In particular, the comparison of D_{app} value obtained for DCE sorption from 100 ppm aqueous solutions shows that for a low sulfonation degree (S = 10%) the DCE sorption kinetics increases by 2 orders of magnitude respect to unsulfonated aerogel.

For a 10 ppm solution, we can observe that the DCE apparent diffusivity constant of both sulfonated and unsulfonated aerogels decreases with respect to the values obtained with 100 ppm solutions. This diffusivity dependence from the penetrant concentration is a typical feature of not extremely diluted Fickian systems,[49] which was already observed for the chloroform vapors sorption in unsulfonated s-PS films.[27]

Nevertheless, the benefit of sulfonation is much larger for the 10 ppm DCE solution than for the 100 ppm ones, and the D_{app} value for a 10% sulfonated aerogel is more than 3 orders of magnitude larger than a unsulfonated aerogel.

The observed increase of DCE diffusivity constants is closely related to the fast water sorption in the hydrophilic sulfonated amorphous phase of s-PS aerogels. In fact, due to the water

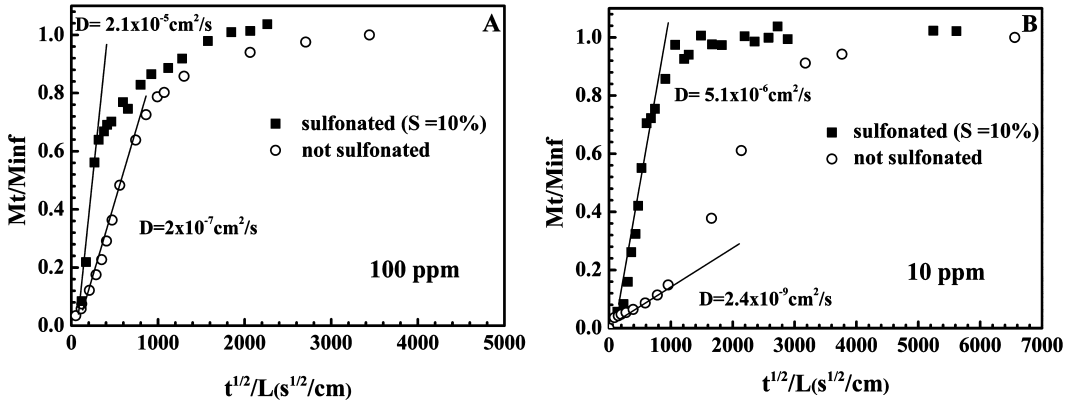

Figure 9. Sorption kinetics at room temperature of DCE from 100 ppm (Figure A) and 10 ppm (Figure B) aqueous solutions for unsulfonated δ-form s-PS aerogels with P = 89% and sulfonated δ-form s-PS aerogels with P = 85% and S = 10%. Mt is the amount of penetrant sorbed at time t, Minf is the amount of penetrant absorbed at equilibrium, and L is the macroscopic thickness of aerogel.

DOI: 10.1021/am507116e
ACS Appl. Mater. Interfaces 2015, 7, 1318−1326

presence into the amorphous phase, the DCE sorption process is no longer influenced by the DCE diffusivity in the amorphous phase but instead depends only on the DCE diffusivity in the water and in the s-PS nanoporous crystalline phase, in which the DCE is absorbed.

In particular, the DCE diffusivity in water (1.05×10^{-5} cm^2 s^{-1}) estimated by Hayduk and Laudie method[53] should be considered as the maximum limit of the DCE diffusivity into the polymer when sorption occurs from aqueous solutions. This value is very close to the observed DCE diffusivity for sorption from 100 ppm DCE aqueous solutions.

CONCLUSIONS

Sulfonated semicrystalline s-PS monolithic aerogels have been prepared using a sulfonation procedure carried out on the gels followed by a solvent extraction by $scCO_2$. This innovative sulfonation procedure allows the preparation of high porosity monolithic aerogels with apparent porosity up to 90% and sulfonation degree up to 30%. Moreover, as the polymer amorphous phase is selectively sulfonated, s-PS aerogels with nanoporous δ crystalline phase are obtained. Thus, monolithic aerogels with high BET values, in the range 250−150 m^2/g are easily obtained, at least for sulfonation degree up to 30%.

Water sorption tests in these sulfonated s-PS aerogels show fast sorption kinetics and high water uptake, associated with reduced aerogel volume variation. In particular, aerogels with sulfonation degree of 15% show water diffusivity comparable to that observed in most common polymeric hydrogels and a water uptake up to 600 wt %. s-PS films having similar sulfonation degree, present water uptake and sorption kinetics 1 and 2 orders of magnitude, respectively, lower than for aerogels.

DCE sorption measurements from aqueous diluted solutions (10 and 100 ppm) have been carried out to investigate a possible use of these innovative materials for water purification applications.

DCE sorption tests of sulfonated s-PS aerogels with a porosity $P \approx 90\%$ and a sulfonation degree $S = 10\%$, show that DCE equilibrium uptake is lower to the uptake of unsulfonated samples (3.2 wt % vs 5 wt % for a 10 ppm aqueous solutions). However, as sulfonated aerogels present much faster DCE sorption kinetics than unsulfonated samples, the sulfonated aerogels are more efficient in DCE sorption from diluted aqueous solutions for short sorption times required for field applications. In particular, the DCE apparent diffusivity constant for a 10 ppm aqueous solution and a sulfonated aerogel with $P \approx 90\%$ and $S = 10\%$ is more than 3 orders of magnitude larger the DCE diffusivity constant for the unsulfonated aerogel with the same porosity. Thus, as a result of the faster kinetics, the DCE uptake in the sulfonated aerogel is ca. 90% of its equilibrium uptake (i.e., ca. 2.9 wt % for an equilibrium uptake of ca. 3.2 wt %) while the unsulfonated aerogel, during the same time, has sorbed only 15% of the equilibrium uptake (i.e., 0.75 wt % for an equilibrium uptake of ca. 5 wt %).

This increase in sorption kinetic is due to high hydrophilicity of the sulfonated amorphous phase, which allows a rapid and direct contact between the DCE dissolved in water and the s-PS nanoporous crystalline δ phase and thus DCE sorption.

In particular, the observed DCE diffusivity for sorption from 100 ppm DCE aqueous solutions is very close to DCE diffusivity in water which can be considered as the maximum limit of the DCE diffusivity into the polymer when sorption occurs from aqueous solutions.

ASSOCIATED CONTENT

Supporting Information

FTIR spectra, SEM micrographs, and BET-IR absorbance correlation. This material is available free of charge via the Internet at http://pubs.acs.org.

AUTHOR INFORMATION

Corresponding Authors

*E-mail: vvenditto@unisa.it.
*E-mail: borriell@unina.it.

Notes

The authors declare no competing financial interest.

ACKNOWLEDGMENTS

The authors thank Prof. Federico Rossi and Dr. Adriano Intiso for the measurements of DCE diffusivity in water. The financial support of the "Ministero dell'Istruzione, dell'Università e della Ricerca" (PRIN 2010 XLLNM3) is gratefully acknowledged.

REFERENCES

(1) Woignier, T.; Phalippou, J.; Zarzycki, J. Monolithic Aerogels in the Systems SiO2−B2O3, SiO2−P2O5, SiO2−B2O3−P2O5. *J. Non-Cryst. Solids* **1984**, *63*, 117−130.
(2) Pierre, A. C.; Pajonk, G. M. Chemistry of Aerogels and Their Applications. *Chem. Rev.* **2002**, *102*, 4243−4266.
(3) Gawel, B.; Gawel, K.; Oye, G. Sol-Gel Synthesis of Non-Silica Monolithic Materials. *Materials* **2010**, *3*, 2815−2833.
(4) Mackenzie, R. C. Clay−Water Relationships. *Nature* **1953**, *171*, 681−683.
(5) Chen, H.-B.; Chiou, B.-S.; Wang, Y.-Z.; Schiraldi, D. A. Biodegradable Pectin/Clay Aerogels. *ACS Appl. Mater. Interfaces* **2013**, *5*, 1715−1721.
(6) Chen, H.-B.; Wang, Y.-Z.; Schiraldi, D. A. Preparation and Flammability of Poly(vinyl alcohol) Composite Aerogels. *ACS Appl. Mater. Interfaces* **2014**, *6*, 6790−6796.
(7) Pekala, R. W. Organic Aerogels from the Polycondensation of Resorcinol with Formaldehyde. *J. Mater. Sci.* **1989**, *24*, 3221−3227.
(8) Tao, Y.; Noguchi, D.; Yang, C.-M.; Kanoh, H.; Tanaka, H.; Yudasaka, M.; Iijima, S.; Kaneko, K. Conductive and Mesoporous Single-Wall Carbon Nanohorn/Organic Aerogel Composites. *Langmuir* **2007**, *23*, 9155−9157.
(9) Pekala, R. W.; Alviso, C. T.; Lu, X.; Gross, J.; Fricke, J. New Organic Aerogels Based upon a Phenolic-Furfural Reaction. *J. Non-Cryst. Solids* **1995**, *188*, 34−40.
(10) Rigacci, A.; Marechal, J. C.; Repoux, M.; Moreno, M.; Achard, P. Preparation of Polyurethane-Based Aerogels and Xerogels for Thermal Superinsulation. *J. Non-Cryst. Solids* **2004**, *350*, 372−378.
(11) Meador, M. A. B.; McMillon, E.; Sandberg, A.; Barrios, E.; Nathan, G.; Wilmoth, N. G.; Mueller, C. H.; Miranda, F. A. Dielectric and Other Properties of Polyimide Aerogels Containing Fluorinated Blocks. *ACS Appl. Mater. Interfaces* **2014**, *6*, 6062−6068.
(12) Williams, J. C.; Meador, M. A. B.; McCorkle, L.; Mueller, C.; Wilmoth, N. Synthesis and Properties of Step-Growth Polyamide Aerogels Cross-Linked with Triacid Chlorides. *Chem. Mater.* **2014**, *26*, 4163−4171.
(13) Katsoulidis, A. P.; He, J.; Kanatzidis, M. G. Functional Monolithic Polymeric Organic Framework Aerogel as Reducing and Hosting Media for Ag Nanoparticles and Application in Capturing of Iodine Vapors. *Chem. Mater.* **2012**, *24*, 1937−1943.
(14) Gavillon, R.; Budtova, T. Aerocellulose: New Highly Porous Cellulose Prepared from Cellulose−NaOH Aqueous Solutions. *Biomacromolecules* **2008**, *9*, 269−277.

DOI: 10.1021/am507116e
ACS Appl. Mater. Interfaces 2015, 7, 1318−1326

(15) Quignard, F.; Valentin, R.; Di Renzo, F. Aerogel Materials from Marine Polysaccharides. *New J. Chem.* **2008**, *32*, 1300−1310.
(16) Del Gaudio, P.; Auriemma, G.; Mencherini, T.; Della Porta, G.; Reverchon, E.; Aquino, R. P. Design of Alginate-Based Aerogel for Nonsteroidal Anti-Inflammatory Drugs Controlled Delivery Systems using Prilling and Supercritical-Assisted Drying. *J. Pharm. Sci.* **2013**, *102*, 185−194.
(17) Ding, B.; Cai, J.; Huang, J.; Zhang, L.; Chen, Y.; Shi, X.; Du, Y.; Kuga, S. Facile Preparation of Robust and Biocompatible Chitin Aerogels. *J. Mater. Chem.* **2012**, *22*, 5801−5809.
(18) Daniel, C.; Alfano, D.; Venditto, V.; Cardea, S.; Reverchon, E.; Larobina, D.; Mensitieri, G.; Guerra, G. Aerogels with Microporous Crystalline Host Phase. *Adv. Mater.* **2005**, *17*, 1515−1518.
(19) Reverchon, E.; Pisanti, P.; Cardea, S. Nanostructured PLLA−Hydroxyapatite Scaffolds Produced by a Supercritical Assisted Technique. *Ind. Eng. Chem. Res.* **2009**, *48*, 5310−5316.
(20) Guenet, J. M.; Parmentier, J.; Daniel, C. Porous Materials from Polyvinylidene Fluoride/Solvent Molecular Compounds. *Soft Mater.* **2011**, *9*, 280−294.
(21) Cardea, S.; Gugliuzza, A.; Sessa, M.; Aceto, M. C.; Drioli, E.; Reverchon, E. Supercritical Gel Drying: A Powerful Tool for Tailoring Symmetric Porous PVDF−HFP Membranes. *ACS Appl. Mater. Interfaces* **2009**, *1*, 171−180.
(22) Daniel, C.; Vitillo, J. G.; Fasano, G.; Guerra, G. Aerogels and Polymorphism of Isotactic Poly(4-methyl-pentene-1). *ACS Appl. Mater. Interfaces* **2011**, *3*, 969−977.
(23) De Rosa, C.; Guerra, G.; Petraccone, V.; Pirozzi, B. Crystal Structure of the Emptied Clathrate form (δ_e Form) of Syndiotactic Polystyrene. *Macromolecules* **1997**, *30*, 4147−4152.
(24) Petraccone, V.; Ruiz de Ballesteros, O.; Tarallo, O.; Rizzo, P.; Guerra, G. Nanoporous Polymer Crystals with Cavities and Channels. *Chem. Mater.* **2008**, *20*, 3663−3668.
(25) Daniel, C.; Longo, S.; Vitillo, J. G.; Fasano, G.; Guerra, G. Nanoporous Crystalline Phases of Poly(2,6-dimethyl-1,4-phenylene)-oxide. *Chem. Mater.* **2011**, *23*, 3195−3200.
(26) Manfredi, C.; Del Nobile, M. A.; Mensitieri, G.; Guerra, G.; Rapacciuolo, M. Vapor Sorption in Emptied Clathrate Samples of Syndiotactic Polystyrene. *J. Polym. Sci., Polym. Phys. Ed.* **1997**, *35*, 133−140.
(27) Musto, P.; Mensitieri, G.; Cotugno, S.; Guerra, G.; Venditto, V. Probing by Time-Resolved FTIR Spectroscopy Mass Transport, Molecular Interactions, and Conformational Ordering in the System Chloroform−Syndiotactic Polystyrene. *Macromolecules* **2002**, *35*, 2296−2304.
(28) Mahesh, K. P. O.; Sivakumar, M.; Yamamoto, Y.; Tsujita, Y.; Yoshimizu, H.; Okamoto, S. Structure and Properties of the Mesophase of Syndiotactic Polystyrene: IX. Preferential Sorption Behavior of sPS-p-Chlorotoluene Mesophase Membrane in a Mixture of Solvents. *J. Membr. Sci.* **2005**, *262*, 11−19.
(29) Venditto, V.; De Girolamo Del Mauro, A.; Mensitieri, G.; Milano, G.; Musto, P.; Rizzo, P.; Guerra, G. Anisotropic Guest Diffusion in the δ Crystalline Host Phase of Syndiotactic Polystyrene: Transport Kinetics in Films with Three Different Uniplanar Orientations of the Host Phase. *Chem. Mater.* **2006**, *18*, 2205−2210.
(30) Mensitieri, G.; Larobina, D.; Guerra, G.; Venditto, V.; Fermeglia, M.; Pricl, S. Chloroform Sorption in Nanoporous Crystalline and Amorphous Phases of Syndiotactic Polystyrene. *J. Polym. Sci., Part B: Polym. Phys.* **2008**, *46*, 8−15.
(31) Daniel, C.; Zhovner, D.; Guerra, G. Thermal Stability of Nanoporous Crystalline and Amorphous Phases of Poly(2,6-dimethyl-1,4-phenylene) Oxide. *Macromolecules* **2013**, *46*, 449−454.
(32) Pilla, P.; Cusano, A.; Cutolo, A.; Giordano, M.; Mensitieri, G.; Rizzo, P.; Sanguigno, L.; Venditto, V.; Guerra, G. Molecular Sensing by Nanoporous Crystalline Polymers. *Sensors* **2009**, *9*, 9816−9857.
(33) Erdogan, M.; Ozbek, Z.; Capan, R.; Yagci, Y. Characterization of Polymeric LB Thin Films for Sensor Applications. *J. Appl. Polym. Sci.* **2012**, *123*, 2414−2422.
(34) Vaiano, V.; Sacco, O.; Sannino, D.; Ciambelli, P.; Longo, S.; Venditto, V.; Guerra, G. N-doped TiO_2/s-PS aerogels for photocatalytic degradation of organic dyes in wastewater under visible light irradiation. *J. Chem. Technol. Biotechnol.* **2014**, *89*, 1175−1181.
(35) Daniel, C.; Sannino, D.; Guerra, G. Syndiotactic Polystyrene Aerogels: Adsorption in Amorphous Pores and Absorption in Crystalline Nanocavities. *Chem. Mater.* **2008**, *20*, 577−582.
(36) Daniel, C.; Giudice, S.; Guerra, G. Syndiotatic Polystyrene Aerogels with β, γ, and ε Crystalline Phases. *Chem. Mater.* **2009**, *21*, 1028−1034.
(37) Daniel, C.; Longo, S.; Cardea, S.; Vitillo, J. G.; Guerra, G. Monolithic Nanoporous−Crystalline Aerogels Based on PPO. *RSC Adv.* **2012**, *2*, 12011−12018.
(38) Daniel, C.; Longo, S.; Ricciardi, R.; Reverchon, E.; Guerra, G. Monolithic Nanoporous Crystalline Aerogels. *Macromol. Rapid Commun.* **2013**, *34*, 1194−1207.
(39) Figueroa-Gerstenmaier, S.; Daniel, C.; Milano, G.; Vitillo, J. G.; Zavorotynska, O.; Spoto, G.; Guerra, G. Hydrogen Adsorption by δ and ε Crystalline Phases of Syndiotactic Polystyrene Aerogels. *Macromolecules* **2010**, *43*, 8594−8601.
(40) Borriello, A.; Agoretti, P.; Ambrosio, L.; Fasano, G.; Pellegrino, M.; Venditto, V.; Guerra, G. Syndiotactic Polystyrene Films with Sulfonated Amorphous Phase and Nanoporous Crystalline Phase. *Chem. Mater.* **2009**, *21*, 3191−3196.
(41) Dembna, A.; Venditto, V.; Albunia, A. R.; Califano, R.; Guerra, G. Sulfonated Syndiotactic Polystyrene: Sorption of Ionic Liquid in the Amorphous Phase and of Organic Guests in the Crystalline Phase. *Polym. Adv. Technol.* **2013**, *24*, 56−61.
(42) Fasano, G.; Califano, R.; Pellegrino, M.; Venditto, V.; Guerra, G.; Borriello, A.; Ambrosio, L.; Sansone, L. Semicrystalline Proton-Conductive Membranes with Sulfonated Amorphous Phases. *Int. J. Hydrogen Energy* **2011**, *36*, 8038−8044.
(43) Wang, X.; Zhang, H.; Jana, S. C. Sulfonated Syndiotactic Polystyrene Aerogels: Properties and Applications. *J. Mater. Chem. A* **2013**, *1*, 13989−13999.
(44) Song, H.; Carraway, E. R. Reduction of Chlorinated Ethanes by Nanosized Zero-Valent Iron: Kinetics, Pathways, and Effects of Reaction Conditions. *Environ. Sci. Technol.* **2005**, *39*, 6237−6245.
(45) Guerra, G.; Manfredi, C.; Musto, P.; Tavone, S. Guest Conformation and Diffusion into Amorphous and Emptied Clathrate Phases of Syndiotactic Polystyrene. *Macromolecules* **1998**, *31*, 1329−1334.
(46) Orler, E. B.; Yontz, D. J.; Moore, R. B. Sulfonation of Syndiotactic Polystyrene for Model Semicrystalline Ionomer Investigations. *Macromolecules* **1993**, *26*, 5157−5160.
(47) Musto, P.; Tavone, S.; Guerra, G.; De Rosa, C. Evaluation by Fourier Transform Infrared Spectroscopy of the Different Crystalline Forms in Syndiotactic Polystyrene Samples. *J. Polym. Sci., Polym. Phys.* **1997**, *35*, 1055−1066.
(48) Zheng, Q.; Cai, Z.; Gong, S. Green Synthesis of Polyvinyl Alcohol (PVA)-Cellulose Nanofibril (CNF) Hybrid Aerogels and Their Use as Superabsorbents. *J. Mater. Chem. A* **2014**, *2*, 3110−3118.
(49) Narasimhan, B.; Peppas, N. A. The Role of Modelling Studies in the Development of Future Controlled Release Devices. In *Controlled Drug Delivery: Challenges and Strategies*; Park, K., Eds; American Chemical Society: Washington, DC, 1997 pp 529−557.
(50) Doll, K. M.; Vermillion, K. E.; Fanta, G. F.; Liu, Z. Diffusion Coefficients of Water in Biobased Hydrogel Polymer Matrices by Nuclear Magnetic Resonance Imaging. *J. Appl. Polym. Sci.* **2012**, *125*, E580−E585.
(51) Hu, Y.; You, J. O.; Debra, T.; Auguste, D. T.; Zhigang Suo, Z.; Joost; Vlassak, J. J. Indentation: A Simple, Nondestructive Method for Characterizing the Mechanical and Transport Properties of pH-Sensitive Hydrogels. *J. Mater. Res.* **2012**, *27*, 152−160.
(52) Musto, P.; Manzari, M.; Guerra, G. Isothermal Guest Desorption from Crystalline and Amorphous Phases of Syndiotactic Polystyrene. *Macromolecules* **1999**, *32*, 2770−2776.
(53) Hayduk, W.; Laudie, H. Prediction of Diffusion Coefficients for Nonelectrolytes in Dilute Aqueous Solutions. *AlChE J.* **1974**, *20*, 611−615.

DOI: 10.1021/am507116e
ACS Appl. Mater. Interfaces 2015, 7, 1318−1326